DESY Summer Student Program 2007

Towards a Refined Calibration for the HERMES Calorimeter

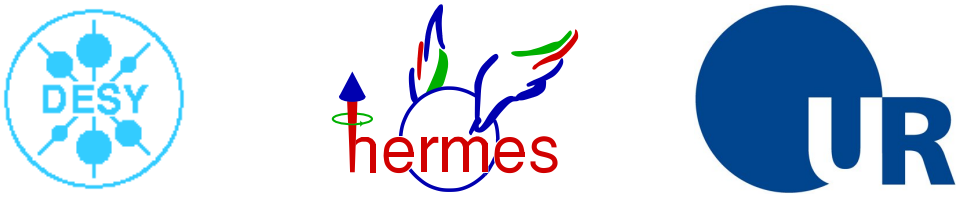

Florian Sanftl

supervised by

E. Avetisyan and A. López Ruiz

September 2007

Contents

1 Introduction

The HERMES electromagnetic calorimeter has been designed to provide a fast first level trigger for the online DAQ, as well as provide PID in the offline analysis by comparing the measured energy deposition in the lead glass blocks with the momentum of the charged tracks reconstructed in the magnetic spectrometer. Besides, it is capable of detecting photons and measuring their energies. As the calorimeter is preceded by a lead-plastic scintillator sandwitch (preshower), part of the energy of the shower does not reach the calorimeter as it's lost in the material of the Pre-Shower. The rough accounting of this losses made during the primary calibration has shown to be insufficient, thus leading to inaccurate values for the measured energy. The functional dependence of the energy losses on momentum and hit position of particles is studied in the current note, with the aim of applying the results in a modernised algorythm of the calibration which will elminate such inaccuracies and allow a better identification of photons produced in exclusive reactions (e.g. the DVCS process).

1.1 Some remarks on the HERA accelerator

The '**H**adron **E**lectron **R**ing **A**ccelrator' HERA was a storage ring of 6.3 km circumference. It was a lepton-proton collider which had the unique feature that both electrons and positrons could be accelerated and stored. Lepton energies up to 27.5 GeV and proton energies of 920 GeV were achieved. The proton beam made use of superconducting magnets to focus and steer the beam. There are two interaction points (IP) where electrons and protons collide, namely in the north and in the south. At these two spots the experiments H1 and Zeus were running. HERA was built between May 1984 and November 1990. On October 19th 1991 the 1st electron-proton collision was observed. From 1995 on, HERMES has been taking data in the East Hall, making use of the electron beam only. Between 1999 and February 2003, HERA-B took data using the proton beam only. During 2001 and 2002 HERA was upgraded with an improved focusing at the collision points, and a better transfer line between the different pre-accelerators.

As the polarisation of the lepton beam is an essential part for HERMES physics the Sokolov-Ternov effect has to be mentioned. This is describing the spontaneous spin-flip process of the leptons in a ring accelerator due to the bending of the partices in the magnetic field. Fermions will automatically aligne their spin parallel or antiparallel to the external magnetic field. Inintially a beam will be unporalized, which means that there are as many particels with spin "up" as with spin "down". Synchrotron radiation can cause a spin-flip whose probability is dependent on the spin orientation. The flip probability is given by

$$\mathcal{P}(\downarrow\rightarrow\uparrow) \neq \mathcal{P}(\uparrow\rightarrow\downarrow)$$

The spin polarisation itself is given by difference of the number of particles with spin orientation $\uparrow$ from the number of particles with spin orientation $\downarrow$:

$$P = \frac{\mathcal{N}(\uparrow) - \mathcal{N}(\downarrow)}{\mathcal{N}(\uparrow) + \mathcal{N}(\downarrow)}$$

The maximum theoretical value is about 92%. At HERA at Energies of $\sim 27.$ GeV the build up time is roughly 25 minutes with polarisation values of $\sim 60\%$ that were achieved in routine operation.

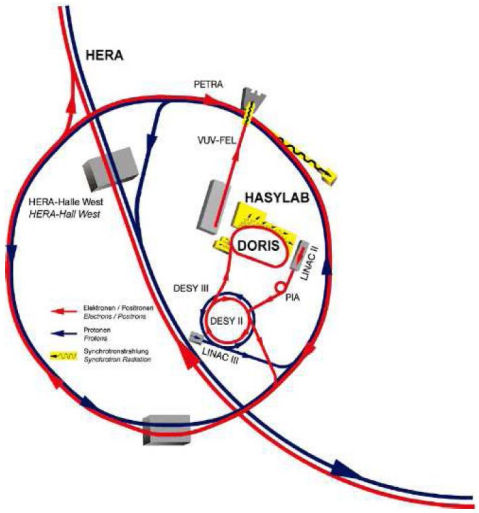

Figure 1: The different Preaccelerators

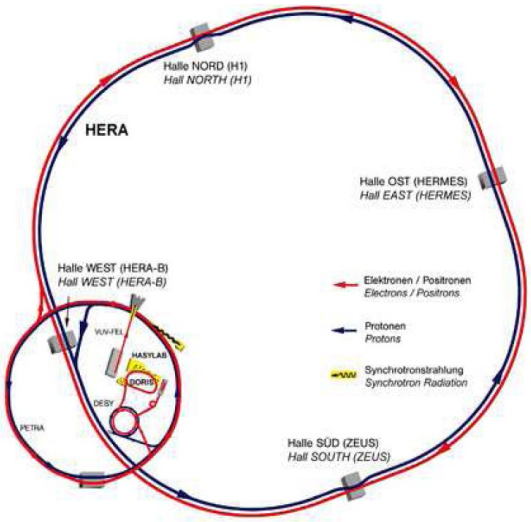

Figure 2: The complete HERA ring

1.2 Deep Inelastic Scattering (DIS) and HERMES Physics

In deep inelastic scattering one collides leptons with high energies (GeV) against nucleons to study the inner structure of the nucleon. This electroweak process is mediated by the exchange of a virtual photon γ^* between the incoming lepton $e^{\pm}$ and the target (nucleons in general, at HERMES most often a proton). At high energies, the wavelengths associated with the leptons are much smaller than the size of the nucleon. Hence the leptons can probe distances that are small compared with the nucleon, so deep within the proton. The scattering is inelastc because the nucleon breaks up after interaction. The reaction products here are the scattered lepton $e'^{\pm}$, the hadronic final state of the nucleon and the produced mesons. One can differ beteween three types of measurements:

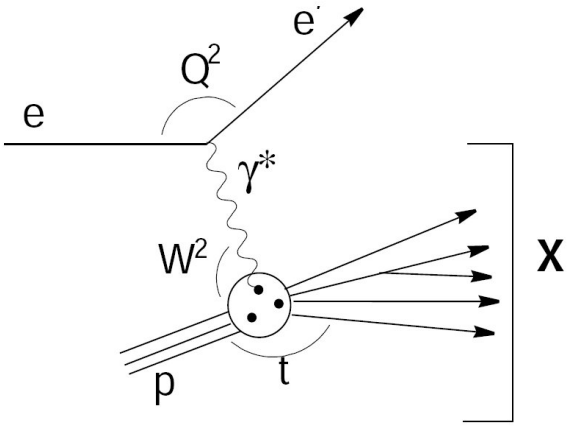

Figure 3: Schematic of a Deep inelastic scattering event

- at **inclusive** measurements one only detects the scattered lepton
- at **semi-inclusive** measurements one detects produced mesons in addition
- at **exclusive** measurements one detects the scattered leptons, the produced mesons and the recoiled nucleon

The following kinematic variables describe a DIS process. In figure 3 the DIS process $e^- + p \rightarrow e'^- + X$ is shwon. The initial and final state of the electron are given by the four-momenta $k = (E, \vec{k})$ and

$k' = (E', \vec{k'})$. The momentum transfer via the virtual photon Q^2 is given by

$$Q^2 = -q^2 = -(k' - k)^2 \sim 4EE'\sin^2(\frac{\theta}{2}) \quad \text{with the assumption} \quad m_e \approx 0$$

The energy of the virtual photon (representing the energy transfer from the lepton to the target) is given by

$$\nu = \frac{P \cdot q}{M} \overset{Lab}{=} E - E'$$

The invariant mass W^2 of all produced hadrons is given by

$$W^2 = P'^2 = (P + q)^2 \overset{Lab}{=} M^2 - Q^2 + 2\nu M$$

where P' is the sum of the four-momenta of all produced particles. M is the mass of the target. For $M^2 = Q^2$ we are in the regime of elastic scattering. In addition, the scattering process depends on so-called scaling variables, namely the fractional energy of the photon with respect to the initial energy

$$y = \frac{P \cdot q}{P \cdot k} \overset{Lab}{=} \frac{\nu}{E}$$

and the Bjorken "x" variable, given by

$$x_B = \frac{Q^2}{2P \cdot q} \overset{Lab}{=} \frac{\nu}{E}$$

This Bjorken "x" longitudinal momentum fraction of quarks in the nucleon. The following are the most common Structure Functions and should be considered as basic knowledge of every HERMES-physicist:

- The **Unpolarized** Strucure Functions F_1 and F_2 describe the cross section of an integrated lepton and target spin. If all participating particles are fermions the following realtion holds $2xF_1(x) = F_2(x)$
- The **Polarized** Strutcure Functions g_1 and g_2 include several combinations of lepton and target spins

HERMES was designed to extract the longtudinal part of the Polarized Structure Functions.

1.3 Overview of the HERMES spectrometer

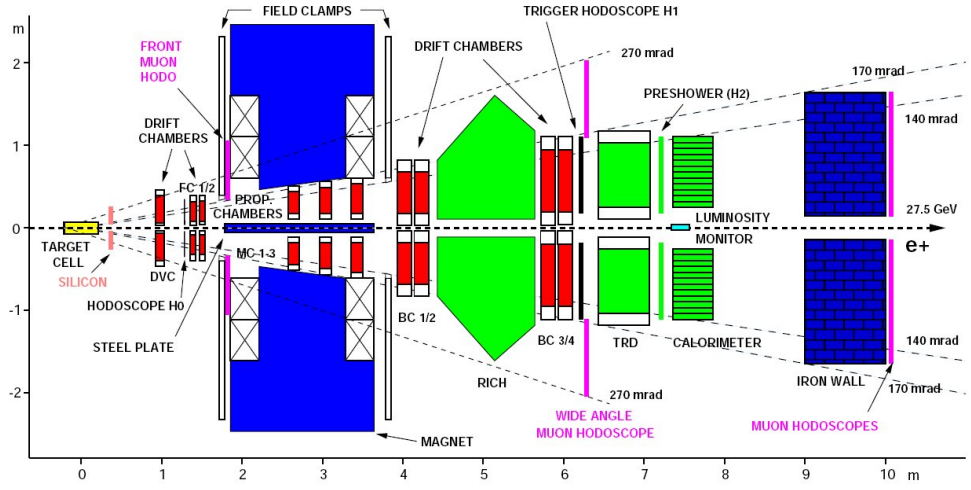

Figure 4: Schematic view of the HERMES spectrometer

HERMES is one of the three experiments at HERA and is located in the East Hall of the HERA facility. It uses the longitudinally polarised electron beam of HERA with unpolarised and polarised gas targets internal to the storage ring. So in contrast to ZEUS and H1 where the lepton and proton beam are brought to collision, HERMES uses a fixed-target configuration. The primary goal of the HERMES experiment is to study the spin structure of the nucleon. The HERMES spectrometer consists of tracking detectors, particle identification detectors and vertical dipole magnet. Apart from the magnet there are tracking chambers after the elliptical target cell (VC, DVC and FC), in the magnet (MC), and before and after the RICH detector (BC). The detectors used for particle identification are the ring imaging Cherenkov detector (RICH) for hadron determination, the transition radiation detector (TRD) for lepton/hadron separation, the Pre-Shower detector the calorimeter for lepton/hadron separation. For further details please refer to the HERMES Spectrometer manual. In the following sections only these elements of the detecor should be described in detail which are directly related to my work, namely the electromagnetic calorimeter and the Pre-Shower.

1.4 The Electromagnetic Calorimeter

Chemical composition	(weight %):
Pb_3O_4	51.23
SiO_2	41.53
K_2O	7.0
Ce	0.2

Physical characteristics:	
Radiation length [cm]	2.78
Density [g/cm^3]	3.86
Critical energy [MeV]	17.98
Refraction index	1.65

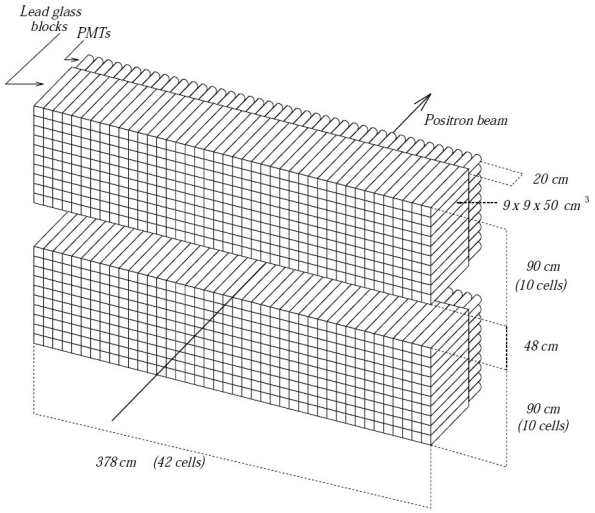

Figure 5: Right: chemical composition of F101; Left: Schematic view of the Electromagnetic Calorimeter

The HERMES calorimeter is built out of 840 identical radiation hard F101 lead-glass blocks each with an area of $9 \times 9\text{cm}^2$, and a length of 50 cm (which sorresponds to $\sim$18 radiation length). Properties of F101 are given in the above table. The block size was chosen in order to contain 99% of an electromagnetic shower inside a matrix of 3×3 blocks. Each block is mirror polished and wrapped in aluminized Mylar foil, and covered with a Tedlar (= Polyvinyl Fluoride) foil to prevent light leakage into neighboring blocks. PMTs are glued to the end of the blocks with a silicon glue. The length of the blocks was optimized to improve the energy resolution. The energy deposition in the lead glass blocks is shown in Figure 5 for muons, electrons and pions. Muons act as minimum ionizing particles. Pions induce a minimum ionizing peak with a long tail due to hadronic showers. Electrons lose nearly all of their energy. The development of electromagnetic and hadronic showers is also schematically shown in Figure 6. The

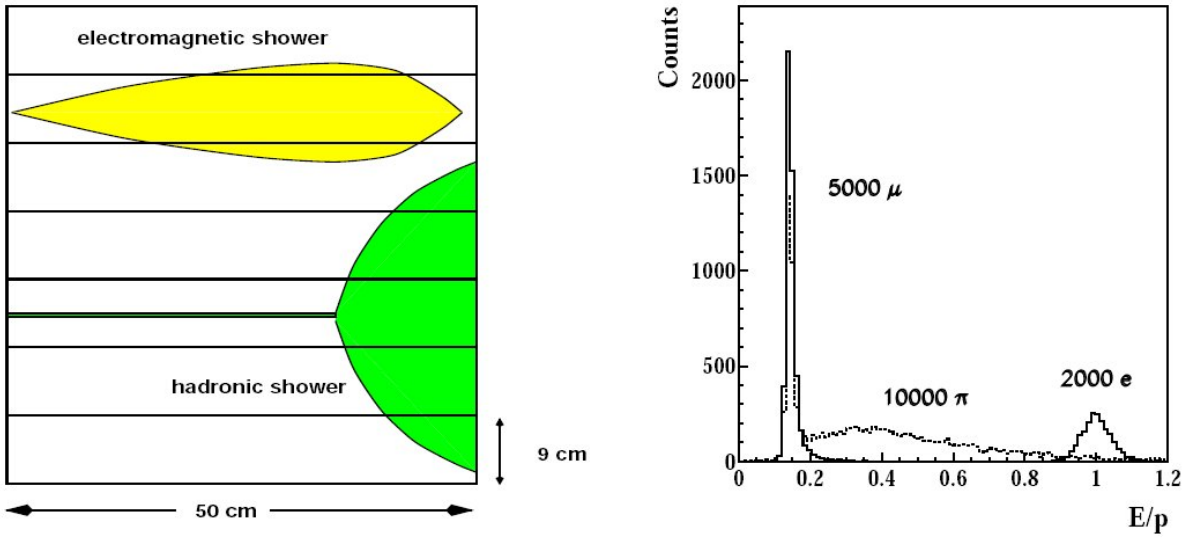

Figure 6: Left: Typical development of an electromagnetic shower; Right: The $\frac{E}{P}$-ratio for muons, pions and elctrons

resoluton of the calorimeter is given by the following parametrization

$$\frac{\sigma(E)}{E}[\%] = \frac{(5.1 \pm 1.1)}{\sqrt{E(GeV)}} + (2.0 \pm 0.5) + \frac{10.0 \pm 2.0}{E(GeV)}$$

which is in practice $\sim 5.2\%$. The E^{-1}-term is due to the Pre-Showering process in the Pre-Shower which improves the discrimination between hadrons and leptons and slightly enhances the the constant term.

1.5 The Preshower

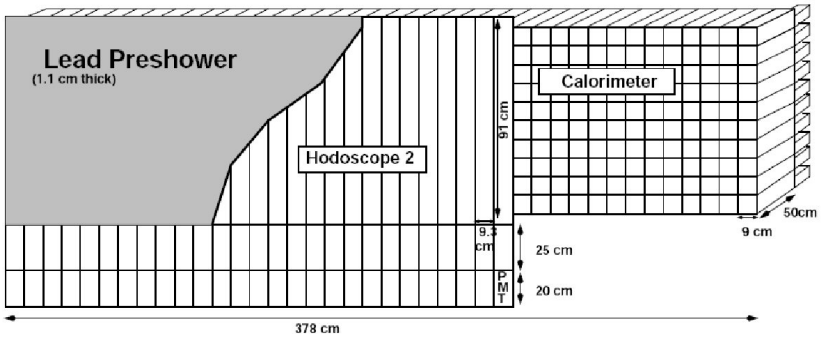

Figure 7: Scheme of the Pre-Shower-module

The Pre-Shower provides first level $e^{\pm}$-trigger signals and particle indentification information. It is composed of 84 vertical scintillator modules (42 each in the upper and lower parts of the detector). The material for the modules is BC-412 from Bicron Co., a fast scintillator with large attenuation length (200-400 cm). The scintillation light is read out with photomultiplier tubes coupled via light guides to the outside ends of the scintillator. The modules are staggered with 3mm of overlap between each unit to increase efficiency. In front of the scintillators (~ 5 cm of distance) there is a 11 mm thick lead block which is sandwiched between 1.3 mm stainless steal plates. This causes a showering process triggered by incident leptons. That way the PID is improved and the trigger efficiency increased. The disadvantage of the showering process is that one has to account energy losses in the lead which is one of the motivations of my project.

2 Towards a refined Calibration

2.1 Motivation for a refined method

The motivation for looking a refined calibration is the $\frac{E}{P}$-ratio of leptons (here only electron, positron!). In the kinematic range of HERMES physics this ratio is constant at 1. But it turns out that it is a funciotn of P. In the follwing histogram one can see the functional dependence of the $\frac{E}{P}$ of the Pre-Shower pulse. The different colors indicate several energetic ranges. The Pre-Shower pulse can be interpreted in the follwoing way: It consists out of a MIP-Signal(=Minimum Ionizing Particle, which corresponds to 2 MeV in plastic) combined with the number of particle which cause the Pre-Shower pulse. It is obviously directly proportional to the number of partcles which are created in the lead and pass through the plastic scintillators. When one applies a linear fit to every momentum bin and draws the fitting values, namely the constant parameter and the slope, in a new histogram one obtains figure 2.1 One can clearly see that the energy losses are more crucial to the lower energy regime than to the hiegher eneergy regime. This is a clear indicator for (more or less constant) energy losses in the detector caused by ionization.

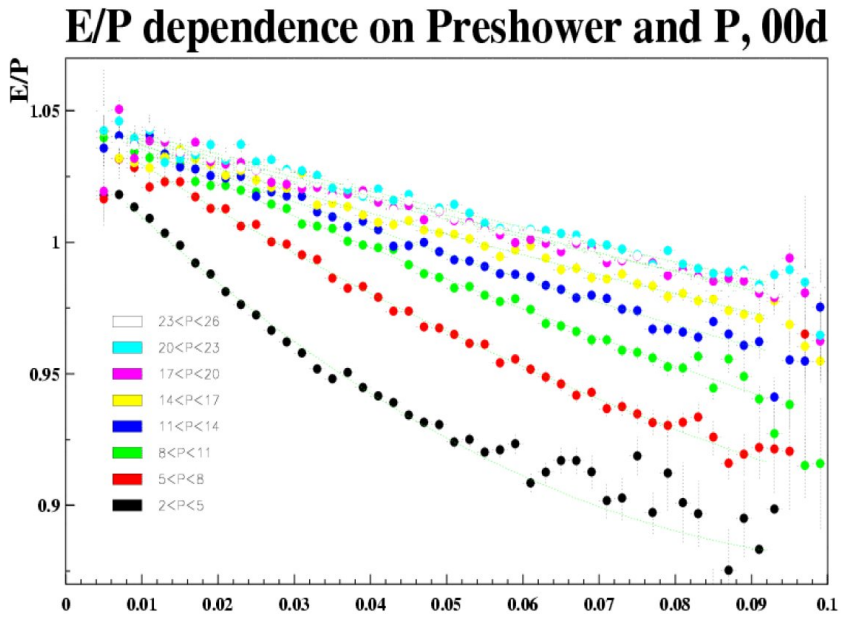

Figure 8: The $\frac{E}{P}$-ratio as a function of the Pre-Shower pulse.

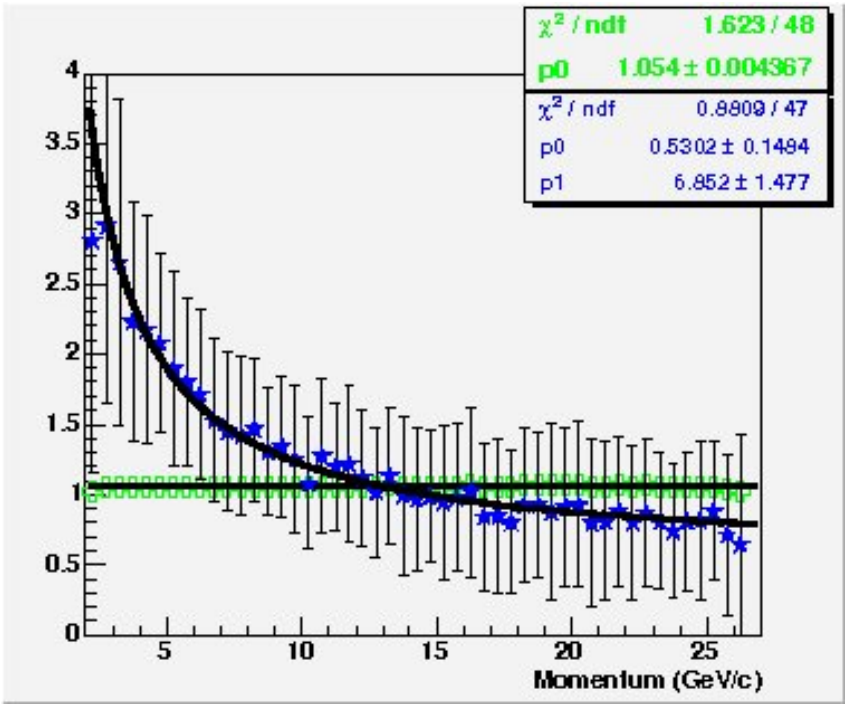

Figure 9: Linear fit parameters to the histogram from above

2.2 The current calibration method

So far the Calibration routine uses the following purely empircal correction factor for the energy measurement:

$$\frac{E_{corr}}{E_{meas}} = A + PulsPre \cdot (B + \frac{C}{E_{meas}}) + \frac{D}{\sqrt{E_{meas}}}$$

It accounts the hperpolic dependence from the Energy like discussed in the chapter before. In adition it combines thie factor with a linear term which takes Pre-Shower pulse into account. Arne Vandenbroucke added the last inversal squareroot term. The motivation for thisterm was also purely empirical, but it turned out to optimize the calibration behaviour which one can clearly see in figure 2.2 that the correction terms decouple the $\frac{E}{P}$-ratio from the energy a bit more, but not yet optimal enough. There is still some place for impovements.

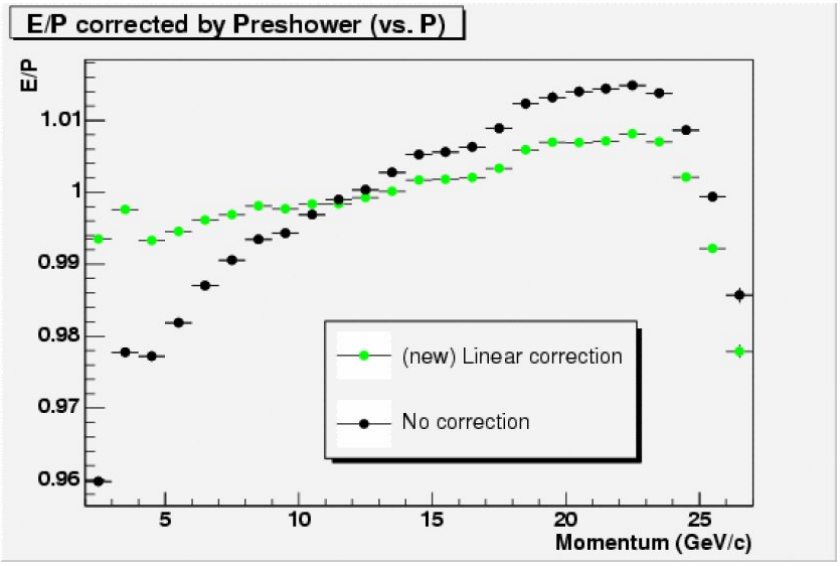

Figure 10: Comparison of the normal calibration with the new claibration

2.3 Monte Carlo Studies

For the Monte Carlo (MC) studies the Rootshower Framework (RSF) has been used. It is part of the ROOT distribution and has been designed to simulate electromagnetic showers through certain tracking media. The chemical and physical properies of the media can be exactly defined. In the original version it only created one event per generation. My modifications split into the following parts:

- create new geometry files which take the exact geometry of the Pre-Shower into account
- define physical properties of the Pre-Shower
- generatation of an arbitrary amount of events
- store the data in a ROOT-tree and present the relevant data after the simulation in a nice overview widget

2.3.1 What is being simulated - an excursus on the theory of electromagnetic showers

For the understanding of the simulation it is more valuable to provide more details on the underlying physical processes than to present thousands lines of source-code. The electromagnetic Calorimeter and Pre-Shower will be discussed in more details as they are the relevant components for this work. First one has to get a general idea what interaction effects may occur when a high energetic particle is

passing through a given material. For high energetic electrons it is mainly Bremsstrahlungs processes, besides ionization processes, for photons though there occur mainly pair splitting processes in a dense nucleus environment (which is in general given by media which are used in calorimaters). The mentioned processes are shown in figure 11 and 12 The radiation length X_0 which is determined by material

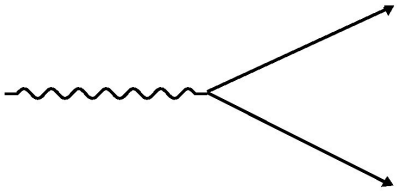

Figure 11: Pair production process

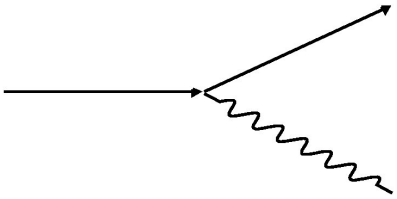

Figure 12: Bremsstrahlungs process

properties is responsible for the longitudinal development of an electromagnetic shower. The transversal spread of a shower is mainly limited due to multiple scattering of the electrons that do not radiate but have a large enough energy to travel far away from the axis. The energy of an electron that loses as much energy in collisions as in radiation has the name of critical energy E_C, so that the natural transverse unit of a shower is the lateral spread of an electron beam of energy E_S after transversing the thickness X_0:

$$R_M = \frac{E_S}{E_C} \cdot X_0 \quad \text{with } E_S = 21\text{MeV}$$

E_S is the usual constant apperaing in multiple scattering theory. The formulae ginig the radiation unit X_0 and the Molière unit R_M are rather complicated. For rapid estimates one can use the approximate expressions

$$\begin{aligned} X_0 &\cong 180 \cdot \frac{A}{Z^2}\frac{g}{cm^2} \qquad \text{for} \quad 13 \leq Z \leq 92 \\ E_C &\cong \frac{550}{Z}\text{MeV} \qquad \text{for} \quad 13 \leq Z \leq 92 \\ R_M &\cong 7 \cdot \frac{A}{Z} \cdot \frac{g}{cm^2} \qquad \text{for} \quad 13 \leq Z \leq 92 \end{aligned}$$

Now, a very simple illustration of the development of an electromagnetic shower shall be shown. Assuming that an elctron is hitting a dense material block it radiates a photon latest after having passed one complete mean free path $< x_free >$. This photon converts after the distance $\frac{7}{9}\langle x_free\rangle = X_0$ into one electron and one positron. These leptons radiata after a certain mean free path agein one photon and so on. After each radiation length the number of particles doubles and the average energy per particle is halved until it reaches the cutoof which is given by the critical energy E_C. When the leptons reach this limit, they start losing their energy by ionization and excitations, the photons by photo effect and compton scattering.

2.3.2 Defining Geometry and the physical/chemical properties of the Pre-Shower and more modifications

The RSF makes use of the `TGeometry`-, `TGeoMedium` and `TGeoMaterial`-package provided by ROOT. The exact definitions of the classes and methods are precisely explained in the ROOT manual and on the ROOT web page. I adapted the definitions to the given geometry of the Pre-Shower. In order to limit the simulation effort I decided to take only the steal-lead-steal-sandwich into account as the ionisation losses in this media are supposed to be highest. The geometry is limited to cover one calorimeter cluster of $27 \times 27\text{cm}^2$ size to further limit the simulation effort. The source code is stored in the `MyDetector.cxx`-File in the `/user/flosan/test/RootShower/`-directory. The results can be seen in the following figure 2.3.2. In order to get an idea how the source-code for one single volume element looks like,the source which defines the properties of the e.g. the lead-block is presented in the following lines.

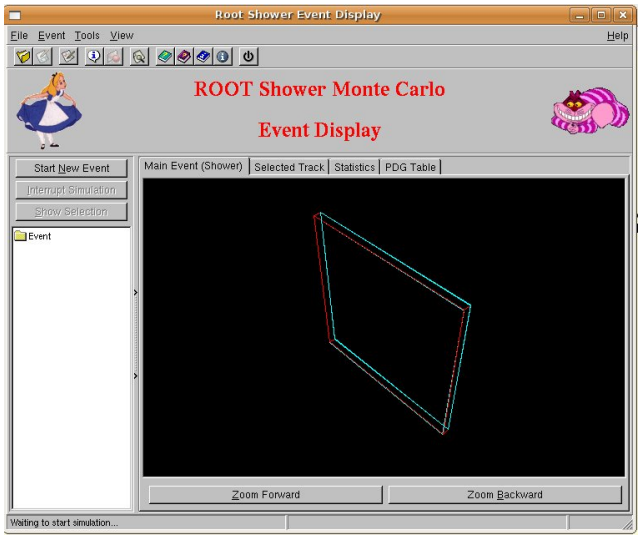

Figure 13: The adapted geometry of the Pre-Shower

```
...
fLead = new TGeoMaterial("Lead",207.2f,82,11.35f,6.37f,194.0f);
...
// lead block of 11mm thickness
fVolume[2] = gGeoManager->MakeBox("BOX1", fDiscriminator, 13.5, 0.55, 13.5);
fVolume[2]->SetLineColor(kRed);
fVolume[2]->SetTransparency(50);
fVolume[2]->SetLineWidth(1);
fVolume[0]->AddNode(fVolume[2],1,fTrans[1]);
...
```

The `TGeoMedium`- and `TGeoMaterial`-classes consider the atomic mass, charge number, the density, the radiation length and the absorbtion-length of the material. The used units correspond to the Particle-Data-Group-conventions. Additionally some automatic data analyzing procedures were implemented (in `RootShower.cxx`).

```
...
    fHisto_npart->Write();
    fHisto_dEdXtot->Write();
    fHisto_ElossvsN->Write();
    //flos final new canvas
    finalStatistics = new TCanvas("Final_Statistics",fi.fFilename,1000,800);
    finalStatistics->Divide(2,2);
    finalStatistics->cd(1);
    fHisto_npart->Draw();
    finalStatistics->cd(2);
    fHisto_dEdXtot->Draw();
    finalStatistics->cd(3);
    fHisto_ElossvsN->Draw();
    finalStatistics->cd(4);
    fHisto_ElossvsN->FitSlicesY();
    fHisto_ElossvsN_1=(TH1D *)gDirectory->Get("EvsN_1");
    if( fHisto_ElossvsN_1 ) fHisto_ElossvsN_1->Fit("pol1");
    // flos riddle
    fHisto_ElossvsN_1->SetXTitle("Number of particles in event");
    fHisto_ElossvsN_1->SetYTitle("Energyloss per event");
    //fHisto_ElossvsN_1->SetXAxis(0.,150);
```

```
22          fHisto_ElossvsN_1->SetMaximum(.5);
23          gStyle->SetOptFit();
24          //finalStatistics->cd();
25          hTree->Write();
26          hTree->Print();
27          epsfile=fi.fFilename;
28          epsfile.Remove(epsfile.Length()-5,5);
29          epsfile+=".eps";
30          finalStatistics->SaveAs(epsfile,"landscape");
31          hfile->Close();
32      ...
```

Here new variables are stored in the Root-tree, and new statistics are generated out of that. In Addition an automatic fit is beeing made. Afterwards all the histograms are stored in an eps-file. One further crucial modification was the method which was responsible for the Bremsstrahlungs calculations. It is called `BremsProb()` and is in the `MyEvent.cxx`-file.

```
1  Double_t MyEvent::BremsProb(Int_t id)
2  {
3     // Check if bremsstrahlung is allowed and generate
4     // a random decay length related to detector's material
5     // radiation length (X0)
6     Double_t p, retval/*, test*/;
7
8     //    if (GetParticle(id)->Energy() > GetParticle(id)->GetMass()) {
9     if (GetParticle(id)->Energy() > 7*GetParticle(id)->GetMass()) {
10       //factor 11 is maybe the right cutoff for the proper amount of particles
11       //test = gRandom->Uniform(1.5,6.);
12       p = gRandom->Uniform(0.2,1.);
13       //test = gRandom->Uniform(0.1,0.3);
14       //p = gRandom->Uniform(test, 1.0);
15       retval = (-fDetector.GetX0(fMatter))*TMath::Log10(p);
16       return (retval);
17    }
18    else return (-1.);
19 }
```

2.3.3 Results

In the following subchapters some results for various parameters are presented. At the end a final conclusion will be made.X

Electron, 5GeV, 15000 events, Bremsprobability $\sim -ln(x)$

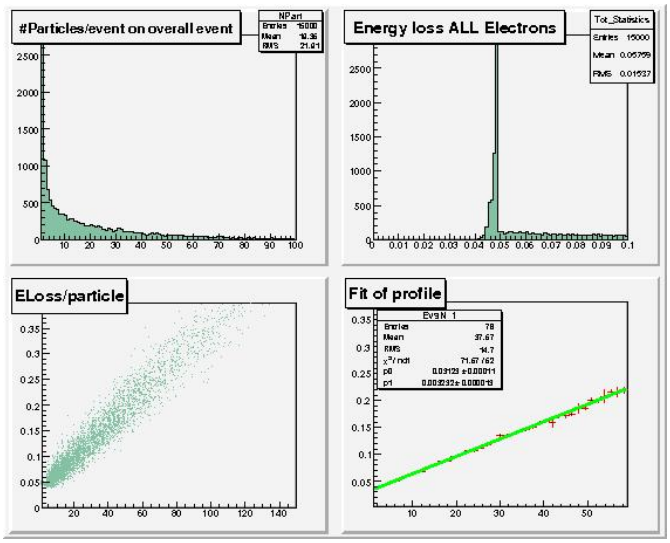

The simulation created a mean value of roughly 20 particles per event. The average energy loss was $\sim$ 58MeV. The smearing of the number of particles/event distribution and the energy loss distriution are not very realistic. The particles/event distribution should have an approximate shape of a Pre-Shower pulse. The energy distribution is too 'peaky' and not widely enough spread. Even though the mean number of particles is in the right range, the energy losses are much too small. They should be roughly in the range of 800 MeV. Due to this bad agreement to the real facts the method which is responsible for the Bremsstrahlungs processes was slightly modified.

Electron, 5-25 GeV, 1000 events, Bremsprobability proportional to $-lg(x)$

For these simulations a certain probability threshold was implemepented in order to produce more Bremsstrahlungs events.

The 5 GeV simulation

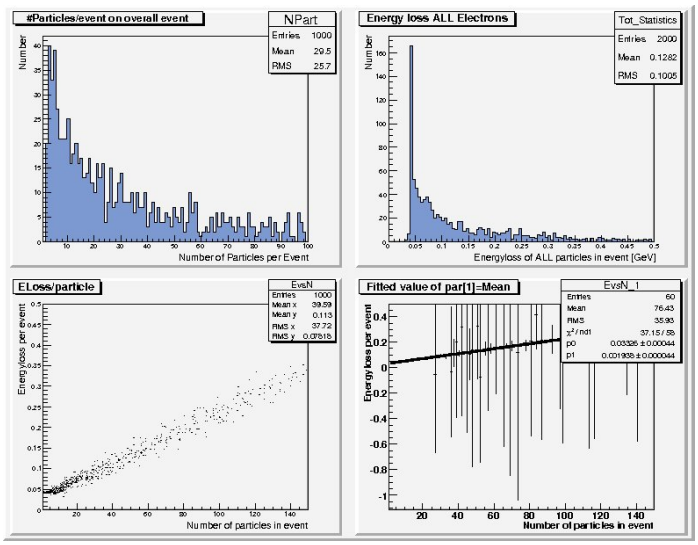

- Mean number of particles per event: ~ 30
- Average energy loss per event: ~ 120 MeV
- particle number distribution: smearing better, although far way from data
- energy distribution: smearing better than befor

The 10 GeV simulation

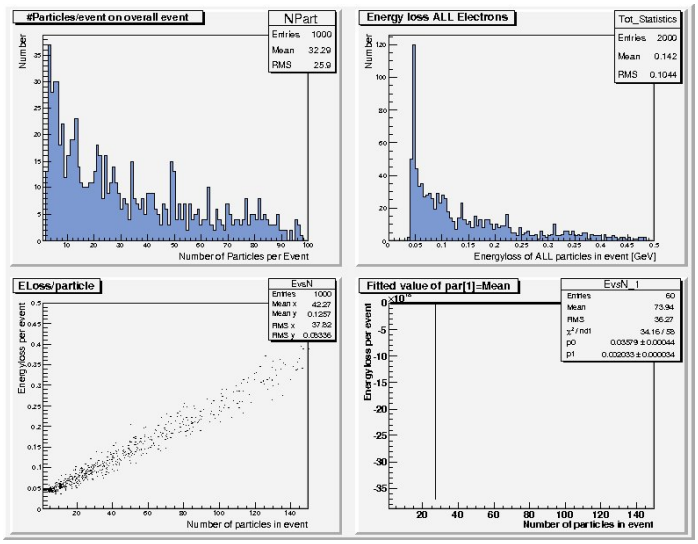

- Mean number of particles per event: ~ 32
- Average energy loss per event: ~ 142 MeV

The 15 GeV simulation

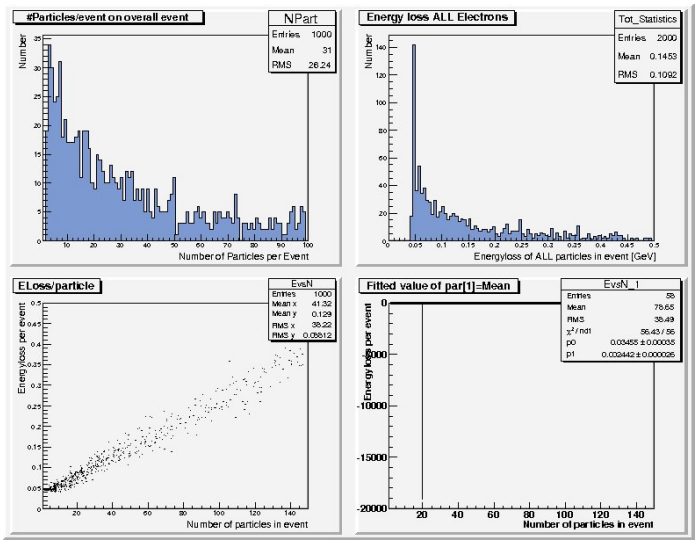

- Mean number of particles per event: ~ 31
- Average energy loss per event: ~ 145 MeV

The 20 GeV simulation

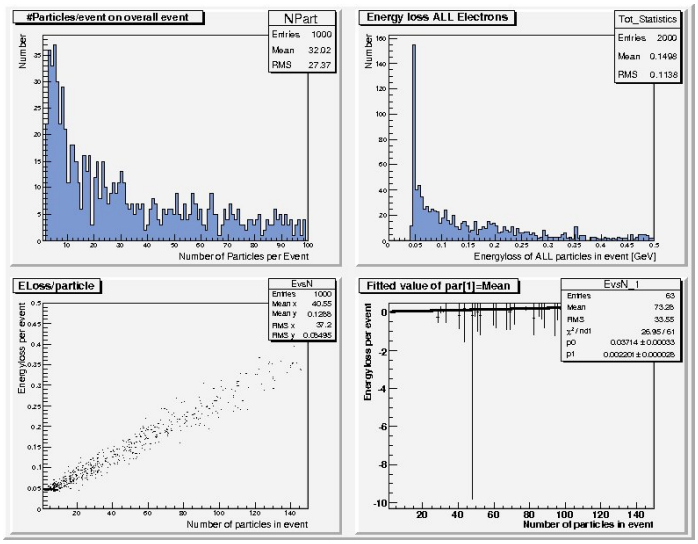

- Mean number of particles per event: ~ 32
- Average energy loss per event: ~ 150 MeV

The 25 GeV simulation

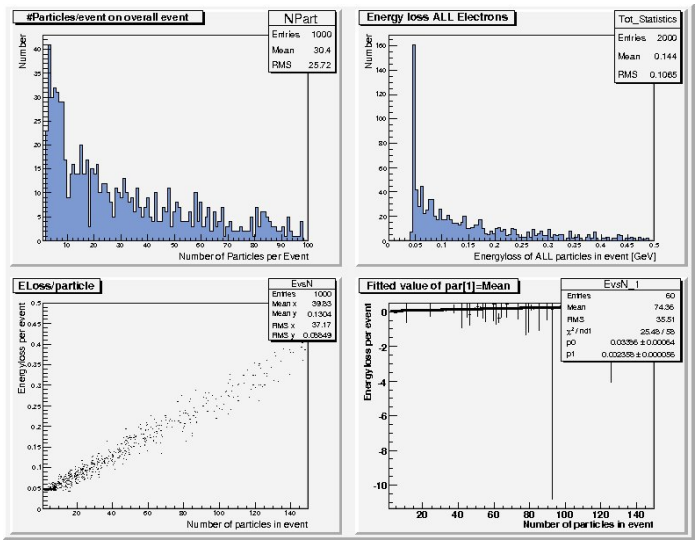

- Mean number of particles per event: ~ 32
- Average energy loss per event: ~ 144 MeV

Photon, 5 and 10 GeV, 1000 events, Bremsprobability proprtional to $-lg(x)$

The 5 GeV simulation

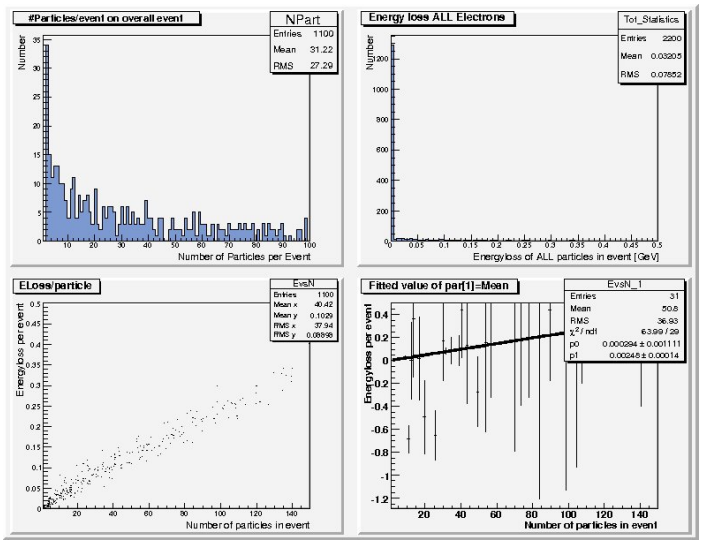

- Mean number of particles per event: ~ 32
- Average energy loss per event: ~ 144 MeV

10 GeV Photon

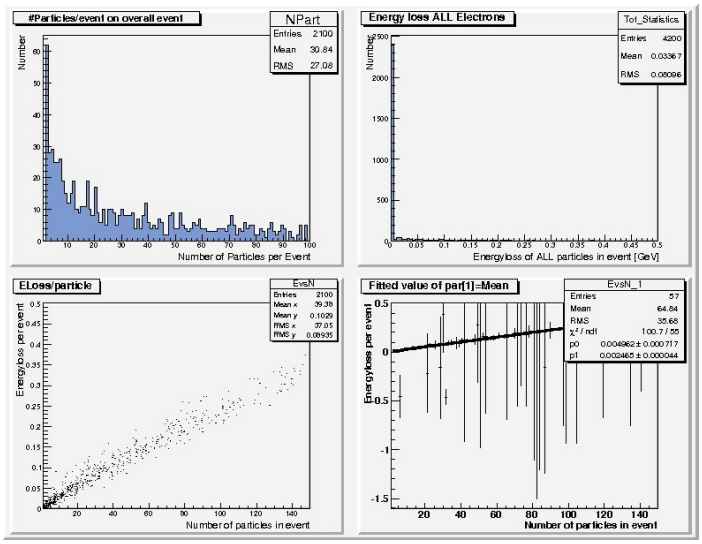

- Mean number of particles per event: ~ 32
- Average energy loss per event: ~ 144 MeV

2.4 An analytical approach

According to Amaldi the number of leptons produced in the shower at the given depth t is described by a Γ function:

$$N(t) = E_0 b \frac{(bt)^{(a-1)} e^{-bt}}{\Gamma(a)}, \tag{1}$$

where a and b are parameters related via $t_{max} = (a-1)/b$ (which corresponds to the maximum penetration depth of an elctromagnetic shower), and $b \approx 0.5$. For every thin slice $t + \Delta t$ the number of (charged) particles produced will be $\Delta N = N(t + \Delta t) - N(t)$. These particles will lose energy for ionisation proportional to the distance from the "birth point" till the end of the lead layer:

$$E_{ion} = C \cdot D \int_{x_0}^{x_{end}} N(t) \cdot (x_{end} - t) dt, \tag{2}$$

where C is the Bethe-Bloch factor of the material and D is the average density of the lead+steel sandwich. By evaluating (numerically by `MAPLE`) the integral function for incident lepton energy of 30GeV, a mean number of charged particles in the shower is found to be ≈ 50, with an ionisation energy loss of ≈ 0.6 GeV which is in a general agreement with data. The histogram which allows to convert the energy distribution into a number of particles is shown in figure 2.4.

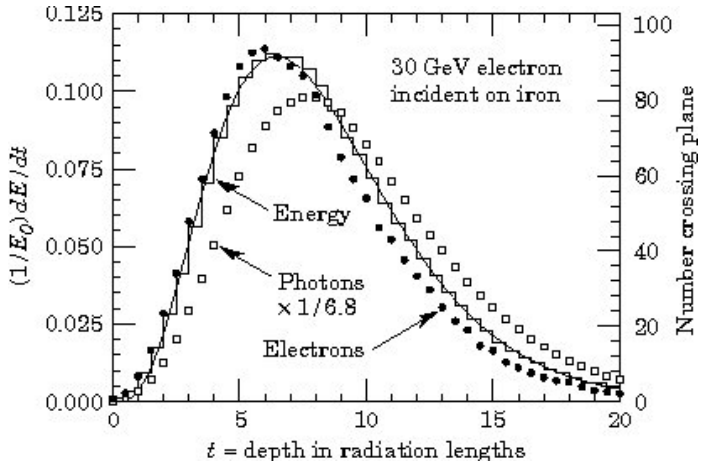

Figure 14: Energy distribution as a function of penetration depth including a conversion scale for the number of particles

3 Outlook and conclusions

The Simulation capability of the Rootshower framework turned out to be too little powerful. It was not possible to find a descriptve for the observed phenomena. This can have several reasons. First one should try in future to implement a `GEANT4` based simulation. One should investigate the analytical part more intensively because this seems to be physically the most motivating contribution to a correction formula. One should completely forget about the simulation capabilities of the Rootshower framework. If the furture investigations will not be successful, a design of an test beam experiment would be considerable. In this experiment a part of the dismantled Pre-Shower hodoscope (H2) and one cluster of Calorimeter blocks could be put into a test beam line here at DESY. One can study different angle dependencies, energy thresholds etc. directly in an experimental setup. One further idea would be to consider the magnetic field at the hodoscope and to make simulations on it.